The correct citation for the paper is:

Chantrasrisalai, C., and D.E. Fisher. 2007. Lighting heat gain parameters: Experimental method. *HVAC&R Research* 13(2):283-303.

Lighting Heat Gain Parameters: Experimental Method (RP-1282)

Chanvit Chantrasrisalai
Student Member ASHRAE

Daniel E. Fisher, PhD, PE
Member ASHRAE

Received June 7, 2006; accepted November 1, 2006

The energy dissipated by lights is a significant contributor to the space heat gain and the space cooling load in many commercial buildings. To account for the heat gain due to lights, both of ASHRAE's new cooling load calculation procedures require the conditioned space/ceiling plenum split and the radiative/convective split as input data. This paper addresses the need to experimentally determine the lighting heat gain parameters for a range of common luminaires under realistic operating conditions. The paper presents both the measurement procedures and the computational procedures required to obtain derived results. The paper also discusses the uncertainty analysis and the accuracy of experimental results and compares different techniques that can be used to obtain the lighting heat gain parameters. Estimated uncertainties in the conditioned space, the ceiling plenum, and the convective fractions are relatively high. These uncertainties vary between ±0.06 and ±0.19. Estimated uncertainties in the shortwave and the longwave radiative fractions are relatively low, varying between ±0.01 and ±0.08 but mostly less than ±0.03. A companion paper presents experimental results along with their estimated uncertainties, discusses the effects of various parameters on the measured results, and provides guidelines for the application of the experimental results.

INTRODUCTION

The heat gain due to lights constitutes a significant contribution to the hourly cooling load in many commercial buildings. Although all of the electrical power input to the lighting system is eventually converted to heat, the transport of lighting energy is very complex, particularly for a recessed luminaire, involving all three heat transfer mechanisms—radiation, convection, and conduction—to two spaces, the conditioned space and the ceiling plenum. Figure 1 illustrates the transport of lighting energy for various luminaires typically used in commercial buildings. The distribution of lighting energy is dependent on numerous variables, including the type of luminaire and lamp, the building construction, the room airflow configuration, and the setpoints of the conditioned space.

In order to account for the heat gain due to lights, both of ASHRAE's new cooling load calculation procedures (Pedersen et al. 1998) use a simple lighting heat gain model. The model requires two lighting heat gain parameters—the conditioned space/ceiling plenum split and the radiative/convective split (Spitler et al. 1997). The conditioned space/ceiling plenum split is the fraction of the lighting power converted to the lighting heat gain of the conditioned space and the fraction of the lighting power converted to the ceiling plenum's lighting heat gain. These fractions are only required for in-ceiling (or recessed) luminaires since it can be assumed that the heat generated by all other luminaires is entirely dissipated in the conditioned space. On the other hand, the radiative/convective split is the fraction of the lighting heat gain of the condi-

Chanvit Chantrasrisalai is a graduate student and **Daniel E. Fisher** is an associate professor in the School of Mechanical and Aerospace Engineering, Oklahoma State University, Stillwater, OK.

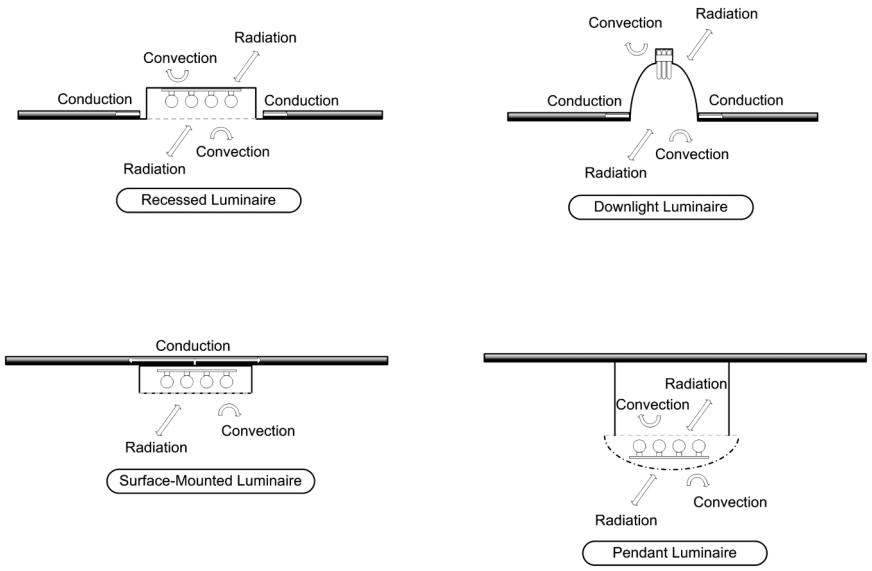

Figure 1. Transport of lighting energy (simplified heat transfer mechanisms).

tioned space that is transferred as radiation and the fraction that is transferred as convection. These fractions are required for both in-ceiling and non-in-ceiling luminaires. In the heat balance (HB) method, the radiative component of the conditioned space lighting heat gain participates in the inside surface heat balance with some prescribed radiative distribution, while the convective component is assumed to go immediately to the air heat balance (i.e., instantaneously becomes cooling load). The HB method treats shortwave and longwave radiation due to lights separately, meaning that shortwave radiation due to lights can be lost from the space through transparent surfaces. The radiant time series (RTS) method, on the other hand, does not distinguish shortwave and longwave radiation. The RTS method uses the so-called nonsolar radiant time factors to convert the radiative component of the conditioned space lighting heat gain into cooling load. Like the HB method, the convective component is assumed to become cooling load immediately.

Published lighting heat gain parameters in the *2005 ASHRAE Handbook—Fundamentals* (ASHRAE 2005) do not present the conditioned space/ceiling plenum "heat gain" split. In addition, the 2005 Handbook data may be obsolete due to recent advancements in lighting technologies. The current research addresses the need to provide relevant lighting heat gain parameters for a range of common luminaires. The lighting heat gain parameters can be economically determined by detailed lighting models (Chung and Loveday 1998a, 1998b; Sowell and O'Brien 1973; Sowell 1990, 1993; Walton 1993). However, these lighting models have only been validated for one type of luminaire considered in the current study, namely, the recessed luminaire with acrylic lens. In addition, the lighting models require appropriate correlations of convection coefficients in order to predict accurate results (Chung and Loveday 1998a, 1998b; Sowell and O'Brien 1973; Sowell 1990, 1993; Walton 1993). Unfortunately, such correlations are not currently available for most luminaires. Therefore, experimental methods are preferable to numerical methods for the current study.

Although similar lighting and thermal performance parameters can be accurately measured using the small-scale calorimeter measurement method (IESNA 2000), the thermal conditions of

the calorimeter do not necessarily reflect those of a realistic building environment, particularly the airflow field within the lamp chamber and around the luminaire. The primary objective of this study is, therefore, to accurately measure the lighting heat gain parameters under realistic operating conditions in a full-scale experimental room. An additional objective of the current study is to provide the experimental results in a format that can be readily applied to the ASHRAE cooling load procedures.

This paper presents an experimental method to determine the lighting heat gain parameters required for cooling load calculations. A companion paper (Chantrasrisalai and Fisher 2007) shows experimental results along with estimated uncertainties, discusses the effects of various parameters on the lighting heat gain parameters, and provides guidelines for the application of the experimental results. Previous studies related to the cooling load effect of lights are discussed in the next section. Following the literature review, the experimental method and the facility and instrumentation are described. Next, the detailed experimental procedures and calculations required to obtain the lighting heat gain parameters are presented. Finally, validation of the experimental method is discussed.

LITERATURE REVIEW

In the past, extensive studies (Ball 1983a, 1983b; Chung and Loveday 1998a, 1998b; Kimura and Stephenson 1968; Mitalas and Kimura 1971; Mitalas 1973a, 1973b; Nevins et al. 1971; Nottage and Park 1969; Rundquist 1990; Sowell and O'Brien 1973; Sowell 1990, 1993; Treado and Bean 1990, 1992) have theoretically and experimentally attempted to analyze and quantify the effect of lights on the cooling load. Among these studies, the work done by Mitalas and Kimura (Mitalas and Kimura 1971; Mitalas 1973a, 1973b) and Treado and Bean (1990, 1992) are of particular interest since they are experimental studies using full-scale test rooms and are therefore directly applicable to the current research. Mitalas and Kimura (1971) used a room-sized calorimeter to determine the cooling load caused by lights. Based on experimental results measured in the calorimeter, Mitalas (1973a, 1973b) later presented design data to estimate the cooling load caused by lights. The design data included room transfer function coefficients (or weighting factors) and the conditioned space/ceiling plenum split. Mitalas's conditioned space/ceiling plenum split is a "cooling load" split, which is different from the "heat gain" split proposed in the current research. Treado and Bean (1990, 1992) describe an experimental study of the interaction between lighting and HVAC systems. They discuss a full-scale test facility similar to Mitalas's calorimeter. They show various lighting and thermal performance parameters, including lighting power consumption, light output, luminous efficacy, cooling load, air temperatures, minimum lamp wall temperature, as well as room transfer function coefficients. However, they provide no information regarding the lighting heat gain parameters. As previously discussed, Mitalas's conditioned space/ceiling plenum split is the cooling load split and, thus, is not applicable to the HB and RTS load calculation methods. The "Validation of Experimental Results" section of this paper compares the proposed conditioned space/ceiling plenum heat gain split with Mitalas's conditioned space/ceiling plenum cooling load split and discusses differences in the two parameters.

OVERVIEW OF TECHNICAL APPROACH

The experimental method required for the present research is based on two distinct experimental techniques: one for the conditioned space/ceiling plenum split and one for the radiative/convective split. The experimental technique for the conditioned space/ceiling plenum split is used for in-ceiling (or recessed) luminaires but is not required for non-in-ceiling luminaires since it is assumed that the heat generated by pendant or ceiling-mounted luminaires is all dissipated in the conditioned space. On the other hand, the experimental technique for the radia-

tive/convective split is used for both types of luminaires. The following sections give an overview of technical approaches used in determining the conditioned space/ceiling plenum split and the radiative/convective split.

The Conditioned Space/Ceiling Plenum Split

The technical approach for estimating the conditioned space/ceiling plenum split is based on the application of the air heat balance to a well-defined control volume. The basic formulation, shown in Equation 1, assumes steady-state, steady-flow conditions and requires measurement of the volumetric flow rate through the control volume and measurement of the air temperatures entering and leaving the control volume.

$$\dot{q}_{ext} = \rho Q C_p (T_{out} - T_{in}) \tag{1}$$

Application of this equation assumes that all heat transfer processes have reached steady state. The approach is applied specifically to two control volumes: the conditioned space and the ceiling plenum. Successful application of the method assumes that the ventilation flow rate and temperatures can be accurately measured. Application of the air heat balance is the primary means of estimating the overall effect of the luminaires on the extraction rate. As previously stated, the conditioned space/ceiling plenum split is a heat gain split, not a cooling load split. However, at steady state, the extraction rate is the same as the cooling load and can be used without loss of generality in the calculation. The difference between the "heat gain" split and the "cooling load" split is that all heat transfer rates (both by extraction and conduction) are included in the calculation of the "heat gain" split, whereas only room and plenum heat extraction rates are used in the calculation of the "cooling load" split. The significance of this difference is explained in more detail in the "Validation of Experimental Results" section of the paper.

The technical approach is similar for both ducted and nonducted returns. The overall heat balance calculation can be determined as the steady-state energy balance of (1) the heat generated in the test room (both plug and light loads), (2) the test room heat extraction rate, and (3) the total steady-state conductive heat transfer between the test room and its guard spaces. For each test with in-ceiling luminaires, the test room with both lights and "plug loads" ON is continuously ventilated until all system, room, and plenum temperatures have reached steady state. The computer interface to the data acquisition system would then continuously plot the overall heat balance error. Once all system, room, and plenum temperatures have reached steady state and the overall heat balance error is acceptably low (typically less than 10% for these experiments), the heat balance of the conditioned space can then be used to calculate the lighting heat gain to the space. Likewise, the plenum heat balance can be used to calculate the lighting heat gain to the ceiling plenum. Detailed calculations of the heat balances are described in the "Experimental Procedure and Calculation" section of this paper.

The Radiative/Convective Split

The technical approach for estimating the radiative/convective split is based on the scanning radiometer measurement technique developed by Hosni and Jones (Hosni et al. 1998; Jones et al. 1998). Jones et al. (1998) show that the radiant heat gain from equipment can be measured by scanning the entire hemisphere around the equipment with a net radiometer. After scanning the hemisphere, the total radiant heat gain can then be determined by summing the product of the radiant fluxes and their associated area over the hemisphere. For the current study, however, the scanning area is a parallel plane covering the luminaires instead of the hemisphere. The technique is used to measure both shortwave and longwave radiation. A net radiometer consisting of four sensors—two pyranometers and two pyrgeometers—is used along with a traversing mecha-

nism to measure the net radiant heat fluxes from the luminaires. The measurement and calculation procedures are also discussed in detail in the "Experimental Procedure and Calculation" section of the paper.

EXPERIMENTAL FACILITY AND INSTRUMENTATION

Description of Experimental Facility

The experimental facility consists of two office-sized test rooms (an upper and a lower test room) located inside a large laboratory space. Each test room is 13.5 × 14.0 × 10.7 ft (4.1 × 4.3 × 3.3 m) and has a commercial raised floor with a floor plenum height of 0.75 ft (0.23 m) as well as a removable commercial suspended ceiling with a ceiling plenum height of 1.79 ft (0.55 m). Although the upper and lower rooms are identical, experimental tests were performed in the lower room, which was instrumented specifically for the lighting experiments. During the experiments, the spaces surrounding the lower test room, including the floor plenums of both the upper and lower test rooms, were configured as temperature-controlled "guard spaces" to minimize conductive heat transfer from the test room. It should be noted that although conductive heat transfer rates are small (the total conductive heat transfer rates for both the conditioned space and the ceiling plenum are less than 5% of the lighting power input for most tests), they all are included in the heat balance calculations to determine the conditioned space/ceiling plenum split. The heat balance calculations are described in the "Experimental Procedure and Calculation" section. The lower test room was sealed from the guard spaces to minimize air leakage and experimental uncertainty. Figure 2 illustrates the experimental configuration used in the measurements.

The walls of the test rooms are constructed of a 2.8675 in. (68.3 mm) expanded polystyrene insulation board sandwiched between white hardboards with an estimated R-value of 11.3°F ·ft^2·h/Btu (2.0 m^2·K/W). The commercial raised floors are made of 0.75 in. (19.1 mm) OSB board. During the tests, the raised floor in the lower test room was covered with linoleum tiles and carpet. The estimated R-value of the raised floor is 2.4°F·ft^2·h/Btu (0.4 m^2·K/W). The floor construction separating the lower and the upper test rooms is composed of 22 gauge steel roof deck and 0.75 in. (19.1 mm) sprayed foam. The floor has an estimated R-value of 5.0°F·ft^2·h/Btu (0.9 m^2·K/W). The acoustic tile suspended ceiling has an R-value of 2.6°F·ft^2·h/Btu (0.5 m^2·K/W).

The test rooms are conditioned by an air-handling system consisting of commercial, variable-speed supply and return fans, a mixing box, cooling and heating coils, and several ASHRAE standard flow measurement boxes. To facilitate a parametric set of experiments, the facility was designed for quick configuration of supply and return ducts/plenums and for quick configuration of ceiling luminaires, diffusers, and grilles. Both ducted ceiling return and ceiling plenum return are supported by the facility.

"Plug Loads" and Lighting Measurement

A watt transducer is used to measure the total heat output generated by the lights under steady-state conditions. Additional watt transducers are used to measure the electrical power of a convective heater (used to represent plug loads), which was included to achieve "typical" steady-state conditions in the room. The presence of the convective heater could have an effect on both the air temperature of the conditioned space and the luminaire performance. To obtain a uniform air temperature in the conditioned space, the convective heater was placed below the supply air diffuser (see Figure 4 for the ceiling configuration) so that the buoyant plume from the heater and the air jet from the diffuser would mix well. Also, the convective heater was oriented in such a way as to avoid direct thermal interaction with the luminaires.

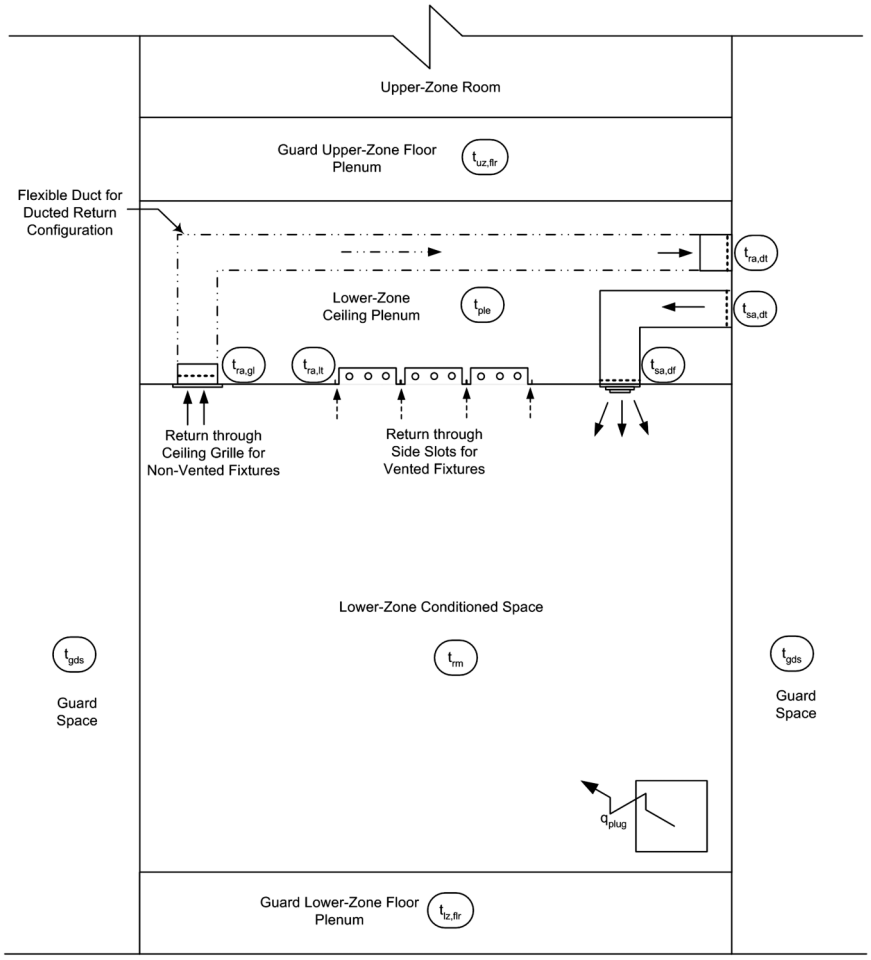

Figure 2. Experimental configuration.

Radiant Heat Gain Measurement

To measure net shortwave and longwave radiant heat gains from the luminaires to the conditioned space, a net radiometer is used. The net radiometer, which consists of two pyranometers and two pyrgeometers, measures net radiant fluxes for both the solar (0.3–2.8 μm) and the far infrared (5–50 μm) spectrums separately. The net radiation measured by the pyranometers represents net shortwave (or solar) radiant flux, and the net radiation measured by the pyrgeometers represents net longwave (or far infrared) radiant flux.

Radiant heat gains are measured by modifying the scanning radiometer measurement technique developed by Hosni and Jones (Hosni et al. 1998; Jones et al. 1998). As previously mentioned, the scanning area is a plane parallel to the luminaires instead of the hemisphere. Figure 3 illustrates scanning radiometer measurements for different types of luminaires. As shown, a scanning area covering luminaires is subdivided into a number of small areas. The net radiometer is automatically moved across the scanning area by a traversing mechanism and records 0.5 minute time-averaged net radiant fluxes for each small area. The 95%

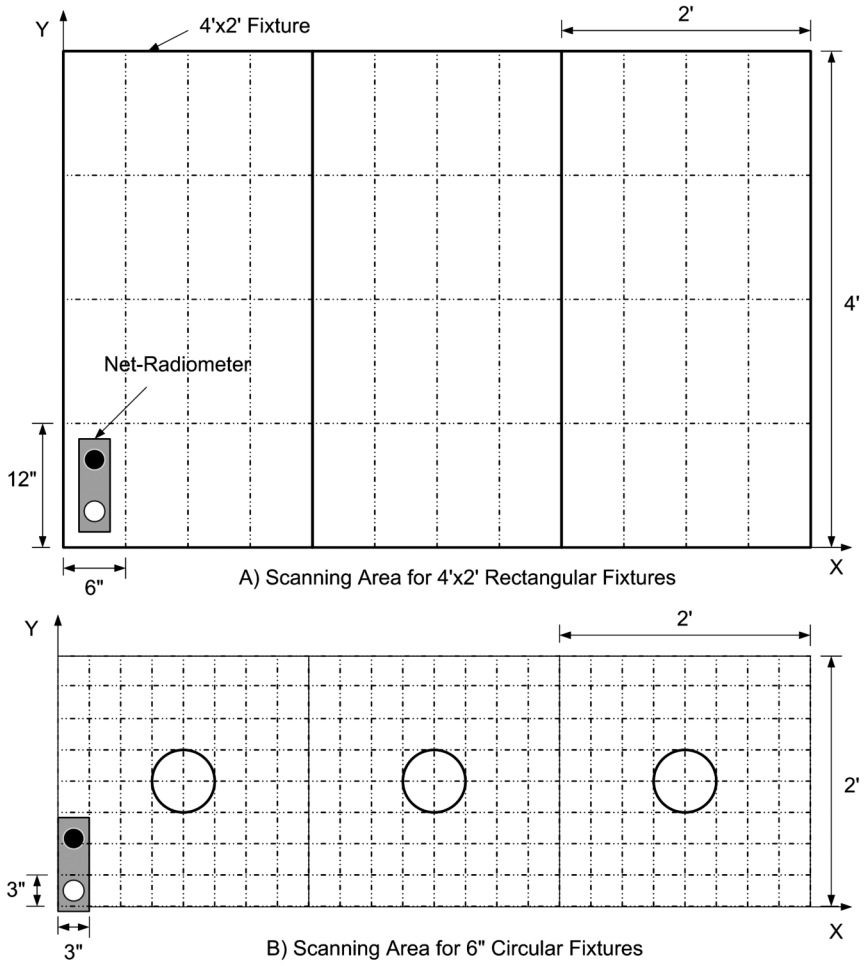

Figure 3. Scanning radiometer measurements.

response time for the pyranometers and pyrgeometers is about 18 seconds. After scanning the entire scanning area, the radiant heat gains from the lights are determined by integrating the fluxes over the scanning area.

As shown in Figure 3, different types of luminaires require different scanning areas and subdivisions. For 2 × 4 ft (0.6 × 1.2 m) rectangular luminaires, a set of radiant heat flux data is collected using one scan with neither the pyranometers nor the pyrgeometers at the center of the measurement area. Based on a sensitivity study, 48 measurement locations with a 6 × 12 in. (0.15 × 0.30 m) subdivision provide sufficiently accurate results with a reasonable scanning time of about 40 minutes.

Unlike the 2 × 4 ft rectangular luminaires, smaller subdivisions are necessary for circular luminaires due to their smaller size. Also, the ceiling area around the circular luminaires is covered with a reflective surface to eliminate any upward radiation (i.e., the upward radiation reflected back through the scanning area) so that the scanning area shown in Figure 3b is applicable. For the circular luminaires, a set of radiant heat flux data is collected using two scans: one scan with the pyranometers at the center of the measurement area and the other scan with the

pyrgeometers at the center. The two scans essentially eliminate the uncertainties due to the positional offset of the sensors but require at least four hours for just one set of data. Based on a sensitivity study, 192 measurement locations with a 3 × 3 in. (0.076 × 0.076 m) subdivision provide sufficiently accurate results for 6 in. diameter circular luminaires.

Heat Extraction Rate and Bulk Air Temperature Measurements

To allow the calculation of heat extraction rates from measured data, the facility is instrumented to measure the volumetric flow rate of the air entering the test room and the temperatures of the air entering and leaving the conditioned space and the ceiling plenum of the lower test room. A flow measurement chamber constructed in accordance with *ANSI/ASHRAE Standard 51-1999, Laboratory Methods of Testing Fans for Aerodynamic Performance Rating* (ASHRAE 1999) is used to measure the air volumetric flow rate. A 4 in. (101.6 mm) throat diameter elliptical nozzle is mounted in the middle of the flow measurement chamber. A differential pressure transducer measures the pressure drop across the flow nozzle. The air volumetric flow rate is then determined according to the procedure given in the standard.

To measure the entering and leaving air temperatures, T-type thermocouples are used. A minimum of four thermocouples are arranged in a grid to allow the calculation of area-weighted average air temperatures. The thermocouple grids are placed in the following locations:

- at the diffuser throat,
- at the side slots of vented luminaires (used for vented luminaires only),
- at the return grille (used for nonvented luminaires for both ducted and nonducted plenum returns), and
- in the ducts at the point where the ducts cross the plane of the plenum (for both supply and return ducts).

Two thermocouple trees measure air temperatures at four elevations in the room. In addition, near-surface temperatures are measured at three locations: near the ceiling, at the center of the walls, and on the guard space side of all room and plenum surfaces. Ceiling plenum temperatures are also monitored by a thermocouple grid in the plenum.

Data Acquisition

Two data acquisition (DAQ) units with precision analog modules are used to obtain all experimental data. All experimental data, except the net radiometer voltages, are scanned at 10-second intervals and transferred to a computer program. The program uses the data to calculate heat balances and displays the desired results on the screen. Both raw and processed data are saved to data files for each particular test once steady-state conditions have been reached. A separate data logging program records the net radiometer voltages along with the measurement location. The program controls the movement of the traversing mechanism and acquires the net radiometer voltages via a DAQ unit. The program then uses the measured voltages to calculate radiant heat gains, which are saved to a separate data file.

EXPERIMENTAL PROCEDURE AND CALCULATION

Experimental Configuration and Procedure

For each of the luminaires described in the companion paper, a full set of data is collected for the carpeted room configuration shown in Figure 2. Figure 4 shows the location of the (2 × 4 ft) luminaires, the supply ceiling diffuser, and the return air grille. The room HVAC system is configured and controlled as follows:

- The conditioned air is supplied through the radial ceiling diffuser.
- The return air is configured for the ceiling plenum return (i.e., nonducted return).
- The airflow rate per floor area is approximately 1.0 cfm/ft^2 (5.1 L/s·m^2).
- The average supply air temperature at the supply air diffuser is maintained between 59.0°F and 62.0°F (15.0°C and 16.7°C).
- The average room air temperature is maintained between 72.0°F and 75.0°F (22.2°C and 23.9°C).

In addition, three variations on the basic room/system test configuration are examined as follows:

- The return air configured for the ducted ceiling return.
- The test room with the no-carpet floor.
- The airflow rate of 0.5 cfm/ft^2 (2.55 L/s·m^2) and 2.0 cfm/ft^2 (10.2 L/s·m^2).

The constant-volume HVAC system is run continuously during the tests. During the warm-up period, the computer program continuously calculates and updates the overall heat balance error as follows:

$$\dot{q}_{err,\,overall} = (\dot{q}_{plug} + \dot{q}_{light}) - (\dot{q}_{ext,\,spc} + \dot{q}_{cond,\,spc\text{-}gds} + \dot{q}_{ext,\,ple} + \dot{q}_{cond,\,ple\text{-}gds} + \dot{q}_{cond,\,ple\text{-}spdct}) \tag{2}$$

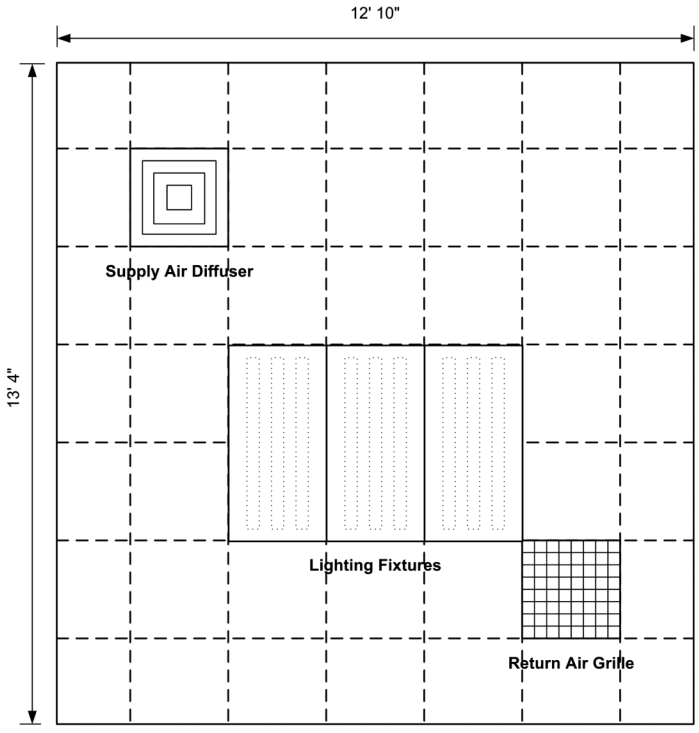

Figure 4. Ceiling configuration.

Power inputs to both the plug loads and the lights are directly measured. The heat extraction rate terms shown in Equation 2 are calculated using Equation 1 with appropriate measured entering and leaving air temperatures. The conductive heat losses/gains between the test room and guard spaces are calculated using the steady-state conduction formulation. It should be noted that conduction terms shown in Equations 2 through 4 are all expressed as conductive heat losses. Estimated R-values of the test room construction are based on thermal properties published in the literature (ASHRAE 2005). The conductive heat loss from the test room ceiling plenum to the supply air duct is estimated as the heat extraction rate of the supply air duct section in the plenum.

When the overall heat balance error is below a specified threshold value (typically 10%) and the operating conditions have reached steady state, measured data (except radiant heat fluxes) are then recorded for at least three hours. Following steady-state data acquisition, the net radiometer traverses its measurement plane collecting fixture radiation data. Two sets of radiant heat flux data are normally collected for each test.

Calculation of the Conditioned Space/Ceiling Plenum Split

Once the overall heat balance error is steady and acceptably low, two possible calculations can be used to determine the lighting heat gain transmitted to the test room's conditioned space. For the first calculation, the lighting heat gain of the conditioned space can be determined directly by performing the conditioned space heat balance calculation as follows:

$$\dot{q}_{light,\,spc,\,1} \approx (\dot{q}_{ext,\,spc} + \dot{q}_{cond,\,spc\text{-}gds} + \dot{q}_{cond,\,spc\text{-}ple}) - \dot{q}_{plug} \tag{3}$$

For the second calculation, the heat balance calculation for the plenum space is first used to determine the lighting heat gain of the ceiling plenum. Then the lighting heat gain of the conditioned space can simply be determined as the difference between the lighting power input and the ceiling plenum's lighting heat gain as follows:

$$\dot{q}_{light,\,ple} \approx (\dot{q}_{ple,\,ext} + \dot{q}_{cond,\,ple\text{-}gds} + \dot{q}_{cond,\,ple\text{-}spdct}) - \dot{q}_{cond,\,spc\text{-}ple} \tag{4a}$$

$$\dot{q}_{light,\,spc,\,2} \approx \dot{q}_{light} - \dot{q}_{light,\,ple} \tag{4b}$$

Typically, the lighting heat gain of the conditioned space calculated by Equation 3 is not the same as that calculated by Equation 4b due to experimental uncertainties (i.e., nonzero overall heat balance error). An average of values determined by Equations 3 and 4 could be used in an estimation of the conditioned space/ceiling plenum split, implying that the weighting parameters W_1 and W_2 in Equation 5 are each 0.5.

$$\dot{q}_{light,\,spc} = W_1 \cdot \dot{q}_{light,\,spc,\,1} + W_2 \cdot \dot{q}_{light,\,spc,\,2} \tag{5}$$

It is likely, however, that the second term of Equation 5 is more accurate than the first term and should be weighted more heavily. There are two reasons to consider this possibility. First, the largest contributor to the nonzero overall heat balance error is likely inaccuracies in the conductive heat transfer rates as discussed in the "Accuracy of Lighting Heat Gain Parameters" section of this paper. Since the uncertainties in the published U-factors are approximately the same for all conduction calculations and since the uncertainty in the measured temperatures are also approximately the same for all conduction calculations, the total conduction contribution to the error scales directly to the conduction surface area. Using this approach, the weighting parame-

ter W_2, which is the ratio of the guarded surface area in the room to the total guarded surface area (room plus plenum), would be about 0.70, and the weighting parameter W_1, which is the ratio of the guarded surface area in the plenum to the total guarded area, would be about 0.3. Second, because the measured air temperatures in the ceiling plenum are typically less uniform than the measured air temperatures in the conditioned space, the fractional errors (i.e., the 70%/30% split) could be adjusted slightly to account for non-uniformity in the air temperatures in the ceiling plenum. With these two considerations, the weighting parameters W_1 and W_2 were selected to be 1/3 and 2/3, respectively, though it should be noted that the difference between the two sets of weighting parameters ($W_1 = 0.33$, $W_2 = 0.67$, and $W_1 = W_2 = 0.50$) were mostly less than 0.05 and were all within the experimental uncertainty range.

After the lighting heat gain of the conditioned space is estimated using Equation 5, the conditioned space fraction is then calculated as a ratio of the conditioned space lighting heat gain to the lighting power input. Finally, the ceiling plenum fraction is simply calculated as one minus the conditioned space fraction. Calculations for ducted and nonducted returns and for vented and nonvented luminaires are similar, with appropriate return air temperatures being used for each particular configuration.

Calculation of the Radiative/Convective Split

The scanning radiometer measurements are used directly to calculate both the conditioned space shortwave and longwave radiant heat gains from the lights as follows:

$$\dot{q}_{rad} = \sum_{i=1}^{n} q''_{rad,\,i} \cdot A_i \tag{6}$$

Radiative fractions can then be determined as ratios of conditioned space radiant heat gains to the lighting power input (i.e., total lighting heat gain). Finally, the convective fraction can simply be determined as the difference between the conditioned space fraction and the sum of the radiative fractions.

It is important to note that the radiative and convective fractions presented here are different from the conventional definitions of the convective/radiative split (ASHRAE 2005). Traditionally, the radiative and convective fractions have been defined as the ratio of the conditioned space radiative or convective gain to the conditioned space lighting heat gain (i.e., the sum of the radiative and convective fractions is equal to one). The computational procedure presented in this paper results in radiative and convective fractions that are based on the *total* lighting heat gain (i.e., the sum of the radiative and convective fractions is equal to the conditioned space fraction). Although the experimental data presented in this paper can be used to calculate the conventional convective/radiative split, the use of the total lighting heat gain based radiative/convective split is preferred for two reasons. First, the uncertainty associated with the *total lighting heat gain based* radiative/convective split is independent of the uncertainty associated with the calculation of the conditioned space/ceiling plenum split since separate measurements are used. However, the uncertainty associated with the *conventional* radiative fractions is strongly dependent on the uncertainty associated with the calculation of the conditioned space/ceiling plenum split. The conventionally defined convective/radiative split is less accurate due to the propagation of the typically high uncertainty in the measured conditioned space/ceiling plenum split.

Second, the total lighting heat-gain-based convective/radiative split provides better insight into the physics of the problem. For example, it is found that changing the airflow rate from 0.5 to 2 cfm/ft^2 (from 2.55 to 10.2 L/s·m^2) only results in a difference of 0.02 in the measured

shortwave fraction for all luminaires tested (see detailed results in the companion paper [Chantrasrisalai and Fisher 2007]). This result, which indicates that changing the airflow rate has a trivial effect on the conditioned space shortwave lighting heat gain, is clearly seen in the total lighting heat-gain-based convective/radiative split. On the other hand, using the conventional definitions would result in a difference of more than 0.16 in the measured results. On the basis of the conventional radiative fractions, one might wrongly conclude that changing the airflow rate has a significant influence on the shortwave lighting heat gain.

VALIDATION OF EXPERIMENTAL RESULTS

Experimental Uncertainty

An uncertainty analysis based on the well-known method of Kline and McClintock (1953) is performed to estimate the accuracy of experimental results. The uncertainty in a primary measurement is estimated as the root sum of the square of the uncertainties due to independent sources of error. Primary measured variables include electrical power, radiant heat flux, temperature, and pressure drop. Table 1 summarizes estimated uncertainties in the primary measurements, their sources of error, and sources of information used in the uncertainty analysis.

Uncertainties in the primary measurements are propagated to intermediate calculated variables, which include volumetric flow rate, heat extraction rates, heat conduction rates, radiant heat gains, as well as conditioned space and ceiling plenum lighting heat gains. Uncertainties in these intermediate variables are then propagated to final calculated results (i.e., lighting heat gain parameters). In this research, an uncertainty in a derived variable is approximated according to Beckwith et al. (1993), as shown in Equation 7.

Table 1. Estimated Uncertainties in Primary Measurements

Measured Variable	Sources of Error	Uncertainty	Source of Uncertainty Estimate
Electrical power	Accuracy of sensor	±0.20% of reading	Manufacturer
	Accuracy of DAQ unit	±0.013% of reading + 1.7 mV	Manufacturer
	Voltage fluctuation	±0.04% of mean value	Statistical analysis (95% confidence based on three-hour steady-state data)
Radiant heat flux	Accuracy of sensor	±7% of reading	Manufacturer
	Accuracy of DAQ unit	±0.013% of reading + 8 μV	Manufacturer
	Sensor orientation	±0.5% of measured flux	Geometrical and radiation analysis
Temperature	Thermocouple accuracy, cold junction compensation, and accuracy of DAQ unit	±0.20°F (±0.11°C)	Calibrated data based on calibration procedure described by Hern (2004)
	Temperature fluctuation	±0.02°F (±0.01°C)	Statistical analysis (95% confidence)
	Spatial averaging	Vary depending on particular locations and experiments	Uncertainty analysis according to Spitler (1990)
Pressure drop	Accuracy of sensor and accuracy of DAQ unit	±1.0% full scale	Sensor calibrated against precision manometer

$$u_y = \sqrt{\left(\frac{\partial y}{\partial x_1}u_1\right)^2 + \left(\frac{\partial y}{\partial x_2}u_2\right)^2 + \ldots + \left(\frac{\partial y}{\partial x_n}u_n\right)^2} \quad (7)$$

All uncertainties are calculated on a case-by-case basis. Measured lighting heat gain parameters along with their estimated uncertainties are presented in detail in the companion paper (Chantrasrisalai and Fisher 2007). Based on the uncertainty analysis, the accuracy of measured lighting heat gain parameters is discussed as follows.

Accuracy of Lighting Heat Gain Parameters

For the conditioned space/ceiling plenum split, comparing the magnitude of the overall heat balance error with the magnitude of the estimated total uncertainty indicates the relative precision of experimental measurements and the relative accuracy of experimental results. Figure 5 shows the overall heat balance for all experiments. The figure shows the total electrical power consumption (plug and light heat gains) plotted against the total test room heat gain (heat extraction rates and conduction rates). A diagonal solid line representing an ideal balance is shown along with diagonal dashed lines representing the ±10% balances. The estimated uncertainty of the total test room heat gain is shown as an error bar on each data point. The estimated uncertainty in the total electrical power input is not shown (less than 0.5%). As shown, although all data points lie within the ±10% lines, most of them are below the ideal line, indicating a systematic (bias) error in the overall heat balance calculation. This systematic error is likely due to inaccurate calculations of the conductive heat transfer (a combined effect of estimated U-factor and measured temperatures). As also shown, the error bar of several data points does not touch the ideal line, implying that the uncertainty is slightly underestimated in those cases. For the current study, Equation 5 is used to handle the energy imbalance as discussed in the "Calculation of the Conditioned Space/Ceiling Plenum Split" section of this paper.

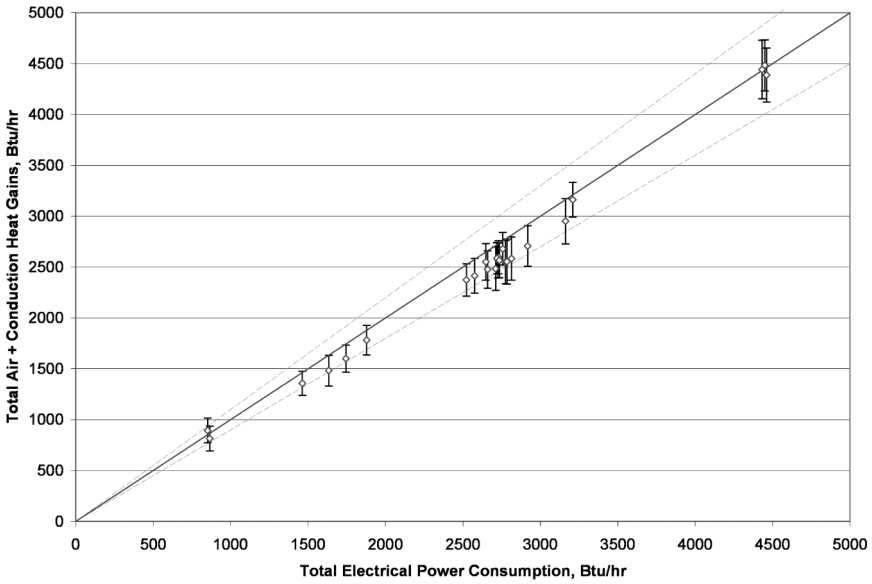

Figure 5. Overall test room heat balance .

As shown in the companion paper (Chantrasrisalai and Fisher 2007), uncertainties in conditioned space, ceiling plenum, and convective fractions are relatively high, varying between ±0.06 and ±0.19. On the other hand, uncertainties in both shortwave and longwave radiative fractions are mostly low, varying between ±0.01 and ±0.03, except for uncertainties in the shortwave fraction for incandescent luminaires. For incandescent luminaires, uncertainties in the shortwave fraction are slightly higher (between ±0.06 and ±0.08) due to higher measured shortwave fractions (between 0.60 and 0.71). It should be noted that although uncertainties in the convective fraction are due to the propagation of both the uncertainty in the conditioned space fraction and the uncertainties in the radiative fractions, they are nearly identical to uncertainties in the conditioned space fraction in most cases since the uncertainty in the radiative fractions is typically trivial compared to the uncertainty in the conditioned space fraction.

High uncertainties in the conditioned space fraction are primarily due to the fact that the total heat gain due to lights is typically less than 50% of the total heat gain generated in the test room. A larger portion of the total test room heat gain is caused by the plug loads used to maintain the test room at typical operating conditions. For instance, although an uncertainty in the conditioned space heat extraction rate is only about ±3% of the space heat extraction rate for a test with 2 cfm/ft^2, the propagation of this uncertainty alone can result in an uncertainty of more than ±15% of the conditioned space lighting heat gain. As shown in the companion paper, uncertainties in the conditioned space fraction for tests with higher airflow rates, which have smaller ratios of lighting heat gain to total heat gain, are typically higher than those for tests with lower airflow rates.

In order to simulate realistic room environments, no extra steps were taken to seal the commercial suspended ceiling and the luminaires. As a result, some air leakage through the ceiling and the luminaires is expected and the average value of the air temperatures measured at the return air grille does not necessarily represent the return air temperature used in the calculations of the conditioned space and ceiling plenum heat extraction rates. Since it was not possible to measure the ceiling leakage rate, the uncertainty due to airflow through the suspended ceiling is not considered in the uncertainty analysis. However, a special test was conducted with a sealed ceiling to investigate its effects. It was found that the sealed ceiling caused a decrease in the conditioned space fraction by about 0.11, which is slightly higher than the estimated uncertainty range (±0.09) for the test. Nonetheless, the sealed ceiling caused an increase in the temperature difference between the plenum and the conditioned space of about 0.5°F (0.28°C). The increase in the temperature difference (higher temperature in the plenum) was a good indication of an increase in the ceiling plenum fraction (i.e., a decrease in the conditioned space fraction).

Comparisons with Published Data/Different Technical Approaches

As illustrated in the companion paper, all lighting heat gain parameters, except the shortwave fraction, are noticeably dependent on room airflow configurations and conditions. This indicates that meaningful comparisons with published data based on small-scale calorimeter tests are difficult to make since thermal conditions in the full-scale room and in the small-scale calorimeter are different. However, it is useful to compare the shortwave fraction with published data since the shortwave fraction is only strongly dependent on lamp types. According to IESNA (2000), a T-8 fluorescent lamp of cool white color converts about 24% of the electrical power input into visible light, while incandescent lamps convert only about 10% to 14% depending on their wattage. For the current study, the measured shortwave fraction for T-8 fluorescent luminaires varies between 0.16 and 0.22, which is close to the published data. The slightly lower value in the measured data indicates losses in the luminaires depending on their design features (i.e., reflector, diffuser, lens, etc.). On the other hand, the measured shortwave fraction for a downlight incandescent luminaire varies between 0.60 and 0.71, depending on lamp types, which is much higher

than the published visible fraction for the incandescent lamps. At first glance, the disagreement appears to indicate a measurement error. However, the pyranometers used in this study measure radiant fluxes in the solar spectrum, which include the entire visible spectrum and a portion of the ultraviolet and the (near) infrared spectrums. This suggests that a large portion of the measured shortwave fraction for incandescent lamps is outside of the visible spectrum, which is indeed the case. As noted in the literature (IESNA 2000), a large fraction of the infrared radiation from an incandescent lamp is in the near infrared region (0.7 to 5 μm). The disagreement between the published visible fraction and the measured shortwave fraction provides a useful reminder of the important difference between visible and solar optical properties of materials.

As implied in the previous discussion, the sensitivity of lighting heat gain parameters to room airflow conditions also argues strongly for full-scale room (rather than calorimeter) experiments. Unfortunately, existing data based on full-scale room experiments are very limited and may not be applicable for the comparison. For instance, Nottage and Park (1969) report some information regarding lighting heat gain parameters for vented luminaires, but their data are not compatible with the current study since their room airflow configuration is completely different (i.e., conditioned air is supplied through plenum having perforated ceiling panels and is returned through luminaires connected to ducted returns). As previously mentioned, Mitalas (1973a, 1973b) presents a conditioned space/ceiling plenum split that is based on cooling loads rather than heat gains. The difference between Mitalas's split and the conditioned space/ceiling plenum "heat gain" split presented in this paper is that all heat transfer rates are included in the calculation of the "heat gain" split, whereas only conditioned space and plenum heat extraction rates are used in the calculation of the "cooling load" split. For the experimental configuration used in the current study, when there is an air temperature difference between the conditioned space and the ceiling plenum, the conditioned space lighting heat gain is equal to the difference between the conditioned space cooling load due to lights (i.e., the conditioned space heat extraction rate minus the plug load) and the conductive heat gain through the ceiling. That is, the heat that first goes to the plenum and then ends up in the conditioned space (i.e., the conductive heat gain through the ceiling) must be subtracted from the conditioned space cooling load due to lights in order to obtain the lighting heat gain of the conditioned space. It is worth noting that all conductive heat transfer rates (e.g., conduction through walls and floors) are accounted for in the calculation of the conditioned space/ceiling plenum "heat gain" split due to imperfect controls. For most experimental tests, the difference between the space "cooling load" fraction and the space "heat gain" fraction is less than 0.10. Typically, the space cooling load fraction is higher due to higher air temperature in the ceiling plenum.

Since no directly comparable measured data for the conditioned space/ceiling plenum split was available, a special test was conducted by first running the room at steady state with the lights turned OFF (but plug loads turned ON) and then switching the lights ON and running the room until steady state was once again reached, this time with the lights ON. The steady-state data for the "lights-off" test was then used to calibrate the steady-state data for the "lights-on" test by assuming that the conditioned space heat balance errors were the same for both tests. This approach is similar to the experimental technique used by Treado and Bean (1990) to calibrate transient cooling loads. It is found that the conditioned space fraction calculated using this technique is about 0.03 less than the fraction determined by the method presented previously in the paper, which is well within the uncertainty range (±0.09) for this test.

As previously mentioned, although detailed lighting models (Chung and Loveday 1998a, 1998b; Sowell and O'Brien 1973; Sowell 1990, 1993; Walton 1993) can be used to predict the lighting heat gain parameters, the models lack the detailed convection correlations required to analyze most of the luminaires tested in the current study. Where natural convection correlations

are applicable, however, the lighting models generate reasonable results. Figure 6 compares measured data for the recessed acrylic lens fluorescent luminaire (i.e., Luminaire #2 shown in the companion paper [Chantrasrisalai and Fisher 2007]) with numerical results from the lighting program developed by Sowell (1989). The theoretical basis of the program can be found in the literature (Sowell and O'Brien 1973; Sowell 1990).

For the experimental configuration shown in Figure 2, the lower-zone test room is modeled with 23 nodes, as illustrated in Figure 7. The numerical test room model is similar to the National Institute of Standards and Technology (NIST) test cell model developed by Sowell (1990). Various input parameters (including convection coefficients, lamp luminous distribution, and power output curve) used to model the NIST test cell were also used for the current study. Power input, room air temperature, and room airflow rate were based on experimental data for the test used in the comparison. Thermal properties were based on data published in the literature (ASHRAE 2005). View factors between nodes were determined using a computer program developed by Walton (2002).

As shown in Figure 6, the solid line (labeled "Measured Data") with error bars represents the measured space fraction and its uncertainty range for the recessed fluorescent acrylic lens luminaire. The measured data are shown as constant since the space fraction was measured at steady state. The dashed line (labeled "Baseline Model") represents the dynamic model result predicted by the lighting program (the lights being turned on at 0.01 hour). As previously discussed, the space fraction of interest is a heat gain fraction, not a cooling load fraction. The conditioned space lighting heat gain used in this paper is equivalent to the "lens downward transport" used in Sowell and O'Brien (1973). In the program, the conditioned space lighting heat gain can be determined as the sum of the convective heat transfer rate from the lens to the room air and the net radiant heat exchange rate between the lens and the room surfaces. As shown in Figure 6, the measured and model results agree quite well with each other. Although the program predicts slightly higher space fractions, they are well within the experimental uncertainty range.

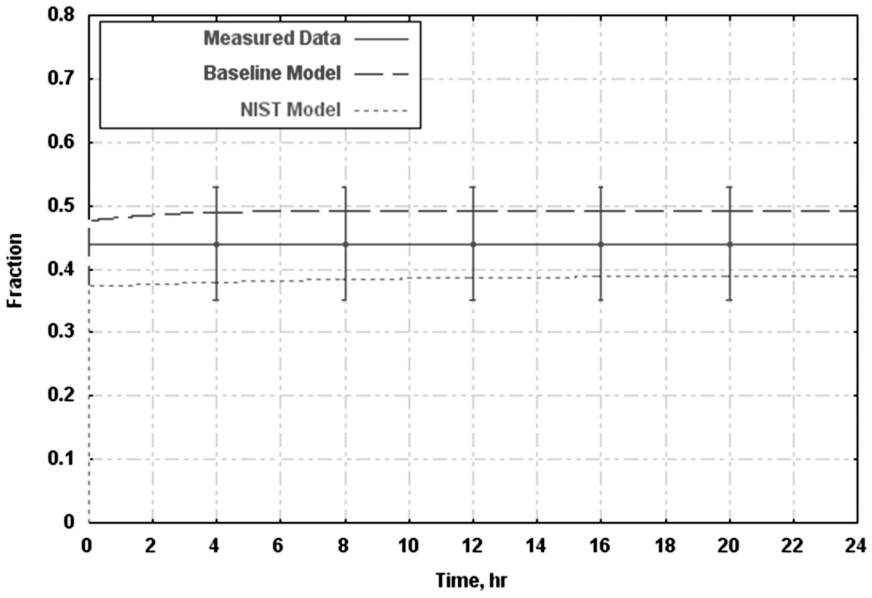

Figure 6. Comparison between measured space heat gain fraction and numerical results.

Figure 6 also shows an additional model result (labeled "NIST Model") represented by the dotted line. The NIST result illustrates the dynamic space fraction for the acrylic lens luminaire with T-12 lamps (40 W) for the NIST test facility. The numerical model of the NIST test facility is described in detail in Sowell (1990). As shown in Figure 6, the measured data and the NIST result also agree well with each other, though the difference between the baseline and NIST model results is quite large. This large difference between the two models could indicate either a sensitivity to model inputs or differences in the total lighting power. The program was used to investigate the sensitivity of lighting heat gain parameters to various model inputs. As shown in Table 2, room-related parameters appear to have a trivial effect on the space fraction, while luminaire-related parameters have a somewhat more significant effect. The sensitivity, however, is not enough to account for the large differences between the baseline and NIST space fractions. It is likely that these are due to the difference in the total lighting power input (the NIST total power input is about twice the baseline total power input) since doubling the total wattage (and room airflow as well) results in the space fraction very close to the NIST result. Comparisons between other lighting heat gain parameters confirm this finding. As shown in Table 2, high total input power ("NIST" case and "Room Airflow Rate and Total Wattage" case) results in low shortwave radiative fraction.

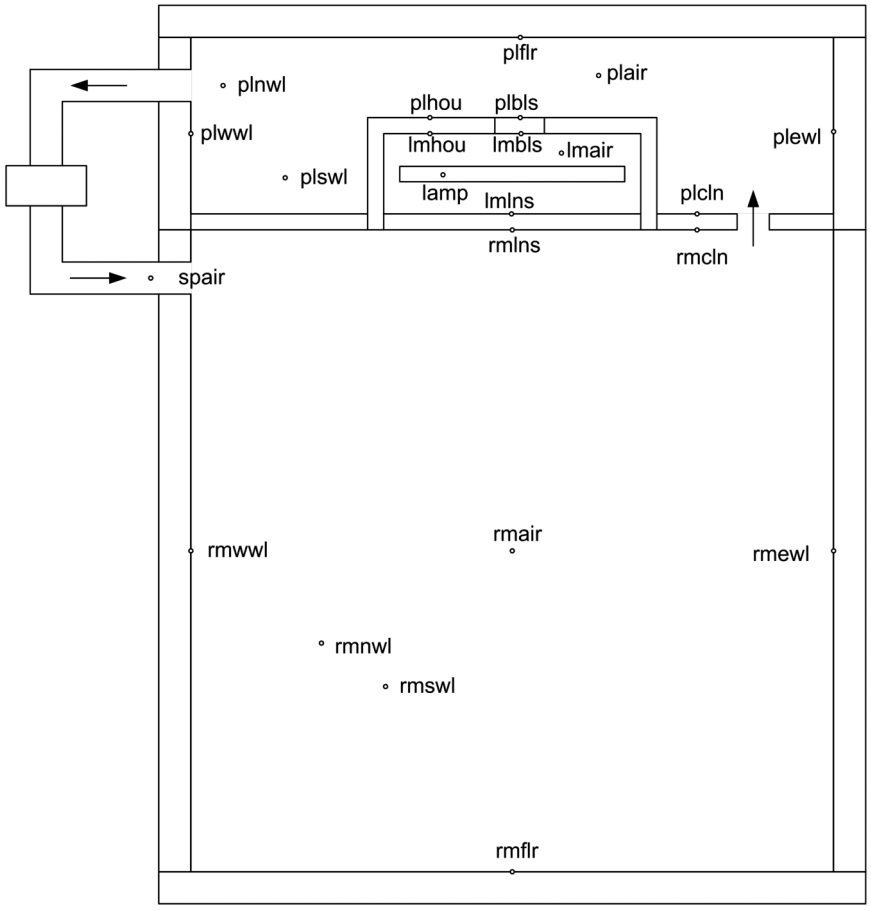

Figure 7. Numerical test room model.

Table 2. Steady-State Results Due to Variations in Input Parameters

Case	Space Fraction	SW Fraction	LW Fraction	Convective Fraction	Change in Input Parameters
Measured data	0.44 ± 0.09	0.20 ± 0.01	0.12 ± 0.01	0.12 ± 0.09	
NIST	0.39	0.12	0.18	0.09	
Baseline model	0.49	0.21	0.19	0.09	
Boundary conditions	0.49	0.21	0.19	0.09	Test room guarded as the NIST study (Treado and Bean 1990)
Room constructions	0.49	0.21	0.19	0.09	Thermal mass of exterior surfaces quadrupled
Room air temperature	0.49	0.21	0.20	0.08	Temperature increased 5°F
Room airflow rate	0.47	0.21	0.18	0.08	Flow rate tripled (PAP tripled)
Convection coefficient	0.48	0.22	0.12	0.14	Convection coefficients tripled (for room and plenum nodes only)
Lamp wattage	0.46	0.16	0.20	0.10	From 32 W lamps to 40 W lamps
Number of lamps per luminaire	0.50	0.22	0.20	0.08	From 4 lamps to 2 lamps per luminaire (both wattage and view factors of luminaire nodes are changed)
Luminaire housing depth	0.47	0.20	0.19	0.08	From 3.1875 in. depth to 5.25 in. depth (housing area and view factors of luminaire and plenum nodes are changed)
Luminaire arrangement	0.49	0.21	0.19	0.09	Luminaires arranged far apart (view factors of room and plenum nodes are changed)
Room airflow rate and total wattage	0.40	0.10	0.20	0.10	Flow rate and total wattage doubled (PAP kept the same as baseline case)

Table 2 also illustrates good agreement between measured data and model results (baseline model) for all lighting heat gain parameters, except the longwave radiative fraction. The difference between measured and model longwave fractions is likely due to the fact that although the natural convection correlations used in the baseline model are suitable for the luminaire nodes, they may not be suitable for the room and plenum nodes since the room airflow rate was quite high (about 7.4 and 33.7 air changes per hour for the conditioned space and the plenum, respectively). As indicated in Table 2, good agreement between measured and model results for all

lighting heat gain parameters can be obtained simply by tripling the convection coefficients for the room and plenum nodes.

It is worth mentioning one particular disagreement between measured and model results, which is the effect of the room airflow rate on the lighting heat gain parameters. As noted in the companion paper, increasing the room airflow rate caused an increase in the measured convective fraction but a reduction in both measured shortwave and longwave fractions for all three tested luminaires. Due to a much larger change in the measured convective fraction, increasing the room airflow rate caused an increase in the measured space fraction. On the other hand, the model results indicate that increasing the room airflow rate causes a reduction in both predicted longwave and convective fractions for the acrylic lens luminaire but a minimal change in the predicted shortwave fraction. A reduction in both longwave and convective fractions results in a reduction in the predicted space fraction. At first, these contradictions may suggest measurement errors and/or model deficiencies. However, a more reasonable explanation is that the room airflow rate may have different effects on the lighting heat gain parameters for different luminaire types due to the fact that all three tested luminaires were luminaires without a lens. This means that the presence of the lens may have an influence on the effect of the room airflow rate since bulk convection between the air in the lamp chamber and the room air typically occurs in the absence of the lens. Further investigations (e.g., numerical models of luminaires without lens or experiments on luminaires with lens) are essential to provide a more credible explanation.

The comparison between measured and model results and the parameter investigation provide several important observations and conclusions. First, measured data and model results agree well with each other. The good agreement supports the validity of the experimental method used in the current study. Second, the predicted space fractions (as well as other lighting heat gain fractions) are somewhat constant within less than an hour after the lights being turned on, as illustrated in Figure 6. These results suggest that the use of constant lighting heat gain parameters measured at steady state is reasonably accurate. Third, the lighting heat gain parameters are quite insensitive to room thermal mass and boundary conditions. These results indicate that the measured lighting heat gain parameters for a particular luminaire can be applied to room constructions and/or boundary conditions that differ from the test room. Last, since detailed lighting models have proven useful in the analysis of lighting heat gain parameters, experimental development of appropriate convection correlations, particularly for luminaires without lens (i.e., bulk convection between the air in the lamp chamber and the room air), should be developed in a full-scale test room.

CONCLUSIONS

This paper presents an experimental method for determining lighting heat gain parameters required by the HB and RTS methods. Two distinct experimental techniques are employed: one for the conditioned space/ceiling plenum split and one for the radiative/convective split. The technical approach for the conditioned space/ceiling plenum split is based on an energy balance applied at steady state to two control volumes: the conditioned space and the ceiling plenum. The technical approach for the radiative/convective split is based on the scanning radiometer measurement technique.

Overall heat balances for all tests are within ±10%. An uncertainty analysis is performed to estimate the accuracy of experimental results and is used as a practical means of validating measured data. Uncertainties in conditioned space, ceiling plenum, and convective fractions are relatively high, varying between ±0.06 and ±0.19. The high uncertainties are due to various factors, including the constraint to maintain the test room environment at typical operating conditions, the difficulty in obtaining a balance between heat generated in the test room and heat removal,

and inherent sensor limitations. On the other hand, uncertainties in both shortwave and longwave radiative fractions are relatively low and are mostly less than ±0.03.

In addition to the uncertainty analysis, the measured data are compared to numerical results from a previously validated detailed lighting program. The measured data agree with the predicted results within the calculated uncertainty associated with the measured data. A sensitivity study using the detailed lighting program indicated that the measured lighting parameters could be applied over a wide range of room constructions and conditions.

ACKNOWLEDGMENTS

This research was sponsored by ASHRAE and directed by the technical committee for cooling and heating load calculations. Peerless Lighting and Gotham Lighting contributed fixtures to the study.

NOMENCLATURE

A	=	area, ft^2 (m^2)
C_p	=	specific heat, Btu/lb·°F (J/kg·K)
n	=	number of measurement locations
$\dot{q}$	=	(net) heat transfer rate, Btu/h (W)
$q"$	=	(net) heat flux, Btu/h·ft^2 (W/m^2)
Q	=	volumetric flow rate, ft^3/h (m^3/s)
T	=	temperature, °F (°C)
u	=	uncertainty
x	=	an independent measured (or intermediate) variable
y	=	the variable derived as a function of independent measured (or intermediate) variables
ρ	=	density, lb/ft^3 (kg/m^3)

Subscripts

cond	=	conduction
err	=	steady-state error
ext	=	extraction rate
i	=	measurement location *i*
in	=	entering air
light	=	lighting gain
out	=	leaving air
overall	=	overall
ple	=	ceiling plenum
ple-gds	=	from ceiling plenum to guard spaces
ple-spdct	=	from ceiling plenum to supply air duct
plug	=	plug load
rad	=	radiant
spc	=	conditioned space
spc-gds	=	from conditioned space to guard spaces
spc-ple	=	from conditioned space to ceiling plenum

REFERENCES

ASHRAE. 1999. *ANSI/ASHRAE Standard 51-1999, Laboratory Methods of Testing Fans for Aerodynamic Performance Rating.* Atlanta: American Society of Heating, Refrigerating and Air-Conditioning Engineers, Inc.

ASHRAE. 2005. *2005 ASHRAE Handbook—Fundamentals.* Atlanta: American Society of Heating, Refrigerating and Air-Conditioning Engineers, Inc.

Ball, H.B. 1983a. The impact of lighting fixtures on heating and cooling loads—Mathematical model. *ASHRAE Transactions* 89(2A):236–58.

Ball, H.B. 1983b. The impact of lighting fixtures on heating and cooling loads—Application to design. *ASHRAE Transactions* 89(2A):259–87.

Beckwith, T.G., R.D. Marangoni, and J.H. Lienhard, V. 1993. *Mechanical Measurements, Fifth Edition*. Reading, MA: Addison-Wesley.

Chantrasrisalai, C. and D.E. Fisher. 2007. Lighting heat gain parameters: Experimental results. *HVAC&R Research* 13(2).

Chung, T.M., and D.L. Loveday. 1998a. Numerical modeling of lighting/HVAC interaction in enclosures—Part I: Light and heat transfer in a room. *HVAC&R Research* 4(1):67–84.

Chung, T.M., and D.L. Loveday. 1998b. Numerical modeling of lighting/HVAC interaction in enclosures—Part II: Effect of including a fluorescent lamp positive column model. *HVAC&R Research* 4(1):85–104.

Hern, S.A. 2004. Design of an experimental facility for hybrid ground source heat pump systems. Master's thesis, Oklahoma State University, Stillwater, OK.

Hosni, M.H., B.W. Jones, J.M. Sipes, and Y. Xu. 1998. Total heat gain and the split between radiant and convective heat gain from office and laboratory equipment in buildings. *ASHRAE Transactions* 104(1A):356–65.

IESNA. 2000. *IESNA Lighting Handbook: Reference and Application, Ninth Edition*. New York: Illuminating Engineering Society of North America (IESNA).

Jones, B.W., M.H. Hosni, and J.M. Sipes. 1998. Measurement of radiant heat gain from office equipment using a scanning radiometer. *ASHRAE Transactions* 104(1B):1775–83.

Kimura, K., and D.G. Stephenson. 1968. Theoretical study of cooling load caused by lights. *ASHRAE Transactions* 74(2):189–97.

Kline, S.J., and F.A. McClintock. 1953. Describing uncertainties in single-sample experiments. *Mechanical Engineering* 75:3–8.

Mitalas, G.P., and K. Kimura. 1971. A calorimeter to determine cooling load caused by lights. *ASHRAE Transactions* 77(2):65–72.

Mitalas, G.P. 1973a. Calculating cooling load caused by lights. *ASHRAE Journal* 5(6):37–40.

Mitalas, G.P. 1973b. Cooling load caused by lights. *Transactions of the CSME* 2(3):169–74.

Nevins, R.G., H.E. Straub, and H.B. Ball. 1971. Thermal analysis of heat removal troffers. *ASHRAE Transactions* 77(2):58–64.

Nottage, H.B., and K.S. Park. 1969. Performance of a ventilated luminaire. *ASHRAE Transactions* 75(2):50–70.

Pedersen, C.O., D.E. Fisher, J.D. Spitler, and R.J. Liesen. 1998. *Cooling and Heating Load Calculation Principles*. Atlanta: American Society of Heating, Refrigerating and Air-Conditioning Engineers, Inc.

Rundquist, R.A. 1990. Considerations in developing a transient heat-from-lights design tool. *ASHRAE Transactions* 96(2):787–93.

Sowell, E.F., and P.F. O'Brien. 1973. The transport of lighting energy. *ASHRAE Transactions* 79(2):172–82.

Sowell, E.F. 1989. *LIGHTS User's Guide—A Computer Program for Modeling of Thermal and Luminous Aspects of Building Lighting Systems*. Department of Computer Science, California State University, Fullerton.

Sowell, E.F. 1990. A numerical lighting/HVAC test cell. *ASHRAE Transactions* 96(2):780–86.

Sowell, E.F. 1993. Improved fluorescent lighting models for building energy program. *Proceedings of Building Simulation '93, August 1993, Adelaide, Australia*. International Building Performance Simulation Association.

Spitler, J.D. 1990. An experimental investigation of air flow and convective heat transfer in enclosures having large ventilative flow rates. PhD thesis, University of Illinois at Urbana-Champaign, Urbana, IL.

Spitler, J.D., D.E. Fisher, and C.O. Pedersen. 1997. The radiant time series cooling load calculation procedure. *ASHRAE Transactions* 103(2):503–15.

Treado, S.J., and J.W. Bean. 1990. Experimental evaluation of lighting/HVAC interaction. *ASHRAE Transactions* 96(2):773–79.

Treado, S.J., and J.W. Bean. 1992. The interaction of lighting, heating and cooling systems in buildings, NISTIR-4701. Technical report, National Institute of Standards and Technology, Gaithersburg, MD.

Walton, G.N. 1993. Computer programs for simulation of lighting/HVAC interactions, NISTIR 5322. Technical report, National Institute of Standards and Technology, Gaithersburg, MD.

Walton, G.N. 2002. Calculation of obstructed view factors by adaptive integration, NISTIR 6925. Technical report, National Institute of Standards and Technology, Gaithersburg, MD.